

# RSC Advances



This is an *Accepted Manuscript*, which has been through the Royal Society of Chemistry peer review process and has been accepted for publication.

*Accepted Manuscripts* are published online shortly after acceptance, before technical editing, formatting and proof reading. Using this free service, authors can make their results available to the community, in citable form, before we publish the edited article. This *Accepted Manuscript* will be replaced by the edited, formatted and paginated article as soon as this is available.

You can find more information about *Accepted Manuscripts* in the [Information for Authors](#).

Please note that technical editing may introduce minor changes to the text and/or graphics, which may alter content. The journal's standard [Terms & Conditions](#) and the [Ethical guidelines](#) still apply. In no event shall the Royal Society of Chemistry be held responsible for any errors or omissions in this *Accepted Manuscript* or any consequences arising from the use of any information it contains.

**Oxidative stability and reaction mechanism of lithium bis(oxalate)borate as  
cathode film-forming additive for lithium ion battery**

Yating Wang<sup>1</sup>, Lidan Xing<sup>1\*</sup>, Xianwen Tang<sup>2</sup>, Xiangfeng Li<sup>2</sup>, Weishan Li<sup>1\*</sup>, Bin  
Li<sup>1</sup>, Wenna Huang<sup>1</sup>, Hebing Zhou<sup>1</sup>, Xiaoping Li<sup>1</sup>

1. School of Chemistry and Environment, Key Laboratory of Electrochemical Technology on Energy Storage and Power Generation of Guangdong Higher Education Institutes, Engineering Research Center of Materials and Technology for Electrochemical Energy Storage (Ministry of Education), South China Normal University, Guangzhou 510006, China
2. Guangzhou Institute of Energy of Testing, Guangzhou 510170, China

**Abstract:**

The oxidative decomposition mechanism of lithium bis(oxalate)borate (LiBOB) as a cathode film-forming additive has been investigated using the density functional theory calculation at the B3LYP/6-311++G(d) level, with polarized continuum model. The calculated oxidation potentials of the investigated structures decreased as the following order: carbonate (including isolate EC, PC and DMC) > BOB<sup>-</sup> (isolate) ≈ carbonate-BOB<sup>-</sup> clusters. Charge distribution results show that the electron of the oxidized carbonate-BOB<sup>-</sup> cluster was taken from BOB<sup>-</sup>, indicating the higher oxidation activity of BOB<sup>-</sup>. Decomposition mechanism analyses of EC-BOB<sup>-</sup>-e cluster indicate that breakage of the BOB<sup>-</sup> structure is energetically favorable than EC. The most likely reaction path of this cluster is the ring opening reaction of BOB<sup>-</sup> via two transition states, generating CO, CO<sub>2</sub> and radical R1, which may further terminates generating borate-containing oligomer. This oligomer is believed to play a crucial role in suppressing further oxidative decomposition of carbonate solvents.

**Key words:** lithium ion batteries; lithium bis(oxalate)borate; oxidative decomposition; film-forming; density functional theory

**1. Introduction**

Lithium ion battery has been widely applied in power portable electronic devices due to its high energy density and high power density. Developing affordable battery offering high reliability, low price and high capacity is becoming the biggest

challenge to expanding the application range of lithium ion battery in electric vehicles [1,2,3,4]. One of the most effective ways to improve the cyclic stability of the battery is to improve the stability of the electrode/electrolyte interface, which can be achieved by forming a protective solid electrolyte interface (SEI) film on the electrode surface [5,6,7,8].

Traditional electrolyte consists of carbonates and lithium hexafluorophosphate ( $\text{LiPF}_6$ ). However,  $\text{LiPF}_6$  has the defects of poor thermal stability generating HF and LiF during the charging-discharging process, which corrode the current collect and increase the interfacial impedance [9,10,11]. Recently, lithium bis(oxalate)borate (LiBOB) aroused people's attention due to its excellent thermal and electrochemical stability [12,13,14,15]. Furthermore, LiBOB has the ability to improve the cyclic performance of the cell by forming an effective protective film on both anode and cathode surface [16,17,18,19]. Specifically, using LiBOB as lithium salt, not only prevents the decomposition of propylene carbonate (PC) on the graphite electrode, but also increases the rate capability of the cell [9]. The reductive decomposition mechanism of LiBOB has been well understood [20]. Importantly, oxidative decomposition of LiBOB also forms a protective film on the cathode surface, improving the cyclic stability of the cell at high voltage [21,22,23,24,25,26]. Ha et al. found that adding 1 wt.% LiBOB into the ethylene carbonate (EC)-based electrolyte generates a stable cathode SEI film, improving the electrochemical performance of Li/LiNi<sub>0.5</sub>Mn<sub>1.5</sub>O<sub>4</sub> cell [26]. There is one small fly in the ointment though, CO and CO<sub>2</sub> gases release during the decomposition reaction of BOB<sup>-</sup>, increasing the internal

pressure of the cells [27].

Up to date, investigations have been focused on the effects of LiBOB on cell performance, while its oxidative stability, film-forming and gas releasing mechanisms are still unclear. The oxidative decomposition of electrolyte on the cathode surface is closely related to the safety issues of lithium ion battery. In our previous works, we have investigated the oxidative stability and decomposition mechanisms of PC and EC by using density functional theory (DFT), and demonstrated that the presence of lithium salt anions ( $\text{PF}_6^-$ ,  $\text{ClO}_4^-$ ,  $\text{BF}_4^-$  and  $\text{B}(\text{CN})_4^-$ ) and neighboring solvents significantly lower the oxidative stability and alter the reaction mechanism of PC and EC [28,29,30,31,32,33,34,35]. In this work, DFT calculations were carried out to understand the oxidative stability, film forming and gas releasing reaction mechanisms of LiBOB.

## 2. Computational details

All calculations were performed using the Gaussian 09 package [36]. The geometry of the investigated structures was optimized using the B3LYP level in conjunction with 6-311++G (d) basis set [37]. Frequency analyses were done with the same basis set to confirm the obtained optimized stationary point. The Gibbs free energy was obtained at 298 K. Vibration frequency and intrinsic reaction coordinate (IRC) analyses were employed to confirm all the transition states of the reaction pathways at the same level. The atomic charge distributions were computed from natural population analysis (NPA) by using natural bond orbital (NBO) theory. To

investigate the role of the electrolyte environment, the bulk solvent effect was estimated using the polarized continuum models (PCM). The acetone dielectric constant (20.5) was used to represent the solvent for PCM calculation. The oxidation potential ( $E_{\text{ox}}$ ) was converted from the absolute oxidation potential of  $\text{Li}^+/\text{Li}$  by subtracting 1.4 V from the former, as shown in eq. (1).

$$E_{\text{ox}}(\text{Li}^+/\text{Li}) = [G(\text{M}^+) - G(\text{M})]/F - 1.4 \text{ V} \quad (1)$$

where  $G(\text{M})$  and  $G(\text{M}^+)$  are the free energy of the solvated complex  $\text{M}$  and its solvated oxidized form  $\text{M}^+$  at 298.15 K, respectively, and  $F$  is the Faraday constant[38].

### 3. Results and Discussion

#### 3.1 Oxidative stability and charge distributions

According to our previous molecular dynamic simulation [39],  $\text{Li}^+$  cations are excluded out of the surface layer electrolyte, while a large amount of solvents and salt anions exist right on the positively charged cathode surface. Hence, oxidative reactions of the isolate solvent, anion, and clusters generating from the solvent and anion were considered in this work. In the LiBOB-containing  $\text{LiPF}_6/\text{carbonate}$  electrolyte, the carbonate solvent may interact with  $\text{BOB}^-$  and  $\text{PF}_6^-$ , generating carbonate- $\text{BOB}^-$  and carbonate- $\text{PF}_6^-$  clusters, respectively. The optimized structures and calculated oxidation potentials of the investigated isolate carbonates (including EC, PC and dimethyl carbonate (DMC)), carbonate- $\text{BOB}^-$  and carbonate- $\text{PF}_6^-$  clusters are presented in Figure 1. The sums of NPA charge distributions of the clusters before

and after oxidation are also given in this figure. It can be seen that the oxidation potentials of the investigated carbonates and clusters decrease as the following order: isolate carbonate > carbonate- $\text{PF}_6^-$  > carbonate- $\text{BOB}^-$ , indicating the lowest oxidation stability of the carbonate- $\text{BOB}^-$  cluster in the investigated electrolytes. This is in agreement with the linear sweep voltammetric results of Ha et al. [26]. As shown in Figure 1, differently with  $\text{PF}_6^-$ , there is no H transfer after the oxidation of carbonate- $\text{BOB}^-$  cluster. The atomic charge distributions of  $\text{BOB}^-$  of isolate  $\text{BOB}^-$  and carbonate- $\text{BOB}^-$  clusters before and after oxidation are summarized in Table 1. It can be seen that the electron is mainly taken from one of the five-ring of  $\text{BOB}^-$  after the oxidation reaction of carbonate- $\text{BOB}^-$ , leading to the breakage of the corresponding C-C bond (from 1.55 to 1.91 Å), while the charge on the carbonate solvent stays constant, confirming the preferential oxidation of  $\text{BOB}^-$ . Next, we focus on the decomposition mechanism of EC- $\text{BOB}^-$  cluster, since EC is the indispensable solvent in the electrolyte [40,41].

### 3.2 Oxidative decomposition mechanism of EC- $\text{BOB}^-$ cluster

For comparison, the oxidative decomposition reaction of isolate  $\text{BOB}^-$  anion was also investigated in this work, as shown in Figure 2. The calculated oxidation potential of  $\text{BOB}^-$  is 5.97V vs.  $\text{Li}^+/\text{Li}$ , which is almost the same with that of EC- $\text{BOB}^-$  cluster, and 1.14 V lower than that of isolate EC. Similarly with the oxidative reaction of EC- $\text{BOB}^-$  cluster, a breakage of C-C bond can be observed after oxidation of the isolate  $\text{BOB}^-$ , as shown in Figure 2. The O-B bond (in the breakage ring of  $\text{BOB}^-$ )

increases from 1.48 to 1.52 Å. Hence, a subsequent breakage of this bond was investigated. It can be found that the oxidized BOB<sup>-</sup> needs only a small energy barrier of 15.75 kJ/mol (TS1) to release CO<sub>2</sub>, which means that gas releasing reaction of the oxidized BOB<sup>-</sup> is easy to take place.

A further decomposition of M1 via C-O bond of another five-ring (TS2,  $\Delta G = 108.23$  kJ/mol) was carried out next. With the breakage of the C-O bond, the five-ring structure was completely destructed generating CO, CO<sub>2</sub> and radical R1, as shown in M2. Gas products of both CO and CO<sub>2</sub> have been detected during the oxidative decomposition of LiBOB-containing electrolyte [26,42]. According to the reaction energy, it is obvious that generating CO<sub>2</sub> is easier than CO.

For EC-BOB<sup>-</sup>-e cluster, there are 7 possible decomposition pathways, as shown in Figure 3, while the corresponding reaction energy was summarized in Figure 4. Decomposition reactions starting from BOB<sup>-</sup> and EC were represented as Path 1 and Path 2 (see Figure 3), respectively. It can be easily found that, except there is a neighboring EC in the cluster, the decompositions of Paths 1 to 3 are similar to those of the isolate BOB<sup>-</sup> (see Figure 2). The existence of the EC solvent does not alter the reaction energy and decomposition products of BOB<sup>-</sup>, as shown in Figure 4. The reaction energy profile of BOB<sup>-</sup> is almost overlapping with that of Path 1 to 3. Decompositions of Path 4 and Path 5 are corresponding to the ring-opening reactions of EC, with the activation energy of 228.4 (TS3-M1) and 231.2 (TS4-M1) kJ/mol, respectively, which are significantly higher than TS1 and slightly higher than TS2. This indicates that further decomposition of the residue structure of BOB<sup>-</sup> in M1 is



kinetically favorable to EC.

As mentioned above, initial decomposition of EC (breakage of C-O bond) in the EC-BOB<sup>-</sup>e cluster is defined as Path 2. The decomposition reaction energy via TS5 is 225.4 kJ/mol, which is higher than all the decomposition reactions of BOB<sup>-</sup> (TS1=19.3kJ/mol, TS2-M1=164.7kJ/mol, TS6-M5=13.92kJ/mol and TS7-M5=207.2 kJ/mol), indicating that the decomposition of EC in EC-BOB<sup>-</sup>e cluster is unfavorable. By comparing the decomposition reactions of EC in Path 2 (TS5), Path4 (TS3-M1=228.4kJ/mol) and Path 5 (TS4-M1 = 231.2kJ/mol), we can find that the participation reaction of BOB<sup>-</sup> (Path 4) has little influence on the decomposition reaction energy of EC.

According to the above discussion, Path 1 to 3 is the most possible while Path 2 to 7 is the least possible decomposition reaction. Additionally, the relative free energy of M3 is 167.4 kJ/mol, which is energetically unfavorable. Hence, the decomposition products of Path 7 (M6) and Path 4 (M3) are not considered in this work.

### 3.3 Termination reactions of radicals

Initial decomposition products of EC-BOB<sup>-</sup>e cluster contain gaseous products, such as CO and CO<sub>2</sub>, aldehyde and radicals R1 and R3. The gaseous products have been found in the oxidative reaction of LiBOB-containing electrolyte [26,42,43,44,45]. Similarly to the decomposition reaction of M1 to M2 (See Figure 3), radical R3 may decompose via a C-O bond in the five-ring structure (See Figure 2, TS 2), generating R1 and gaseous products, CO and CO<sub>2</sub>. Termination reactions of R1 are

investigated, as presented in Figure 5. Two R1 radicals may terminate forming P1, while three R1 radicals generate borate-containing oligomer P3. This kind of borate-containing oligomer has been found on the cathode surface after cycling in the 1 wt. % LiBOB-containing electrolyte, by X-ray photoelectron spectroscopy measurement. And this borate-containing film is believed to play an important role in suppressing further oxidative decomposition of solvents and improving the stability of the electrode/electrolyte interface [26].

#### 4. Conclusions

The reaction mechanisms of LiBOB as cathode film-forming additive have been investigated by density functional theory calculations in this work. Calculated oxidation potentials of the investigated structures decreased as the following order: carbonate (including EC, PC and DMC) > BOB<sup>-</sup> (isolate)  $\approx$  carbonate-BOB<sup>-</sup> clusters. Charge distribution results show that the electron of the oxidized carbonate-BOB<sup>-</sup> cluster was taken from BOB<sup>-</sup>, indicating that BOB<sup>-</sup> is oxidized preferentially to the investigated carbonate solvents. Decomposition reactions of the oxidized EC-BOB<sup>-</sup> cluster show that decompositions of BOB<sup>-</sup> are energetically favorable to EC. The most likely reaction path of this cluster is the decomposition of BOB<sup>-</sup> via two transition states, generating CO, CO<sub>2</sub> and radical R1, which may further terminates generating borate-containing film. All of these oxidative decomposition products are in good agreement with the experimental detections. And the borate-containing film is believed to play a crucial role in suppressing further oxidative decomposition of

carbonate solvents and improving the cyclic stability of the cell.

Additionally, we found that the existence of EC does not alter the oxidative stability and decomposition reaction energy of BOB<sup>-</sup>.

### Acknowledgments:

This work is supported by National Natural Science Foundation of China (21003054, 21273084), the joint project of National Natural Science Foundation of China and Natural Science Foundation of Guangdong Province (Grant No.U1134002), Natural Science Foundation of Guangdong Province (10351063101000001, S2011040001731), Cooperation Project of Industries, Universities and Research Institutes in Guangdong Province (Grant No. 2012A090300012), and the key project of Science and Technology in Guangdong Province (Grant No. 2011A010802001), and the scientific research project of Department of Education of Guangdong Province (2013CXZDA013).

### References

- 
- [1] P. Leung, X. Li, C. P. de León, et al. Progress in redox flow batteries, remaining challenges and their applications in energy storage, *RSC Advances*, 2012, **2**, 10125-10156.
  - [2] T. F. Yi, Y. Xie, L. J. Jiang, J. Shu, et al. Advanced electrochemical properties of Mo-doped Li<sub>4</sub>Ti<sub>5</sub>O<sub>12</sub> anode material for power lithium ion battery, *RSC Advances*, 2012, **2**, 3541-3547.
  - [3] W. He, J. Qian, Y. Cao, et al. Improved electrochemical performances of nanocrystalline Li [Li<sub>0.2</sub>Mn<sub>0.54</sub>Ni<sub>0.13</sub>Co<sub>0.13</sub>] O<sub>2</sub> cathode material for Li-ion batteries, *RSC Advances*, 2012, **2**, 3423-3429.
  - [4] P. Zhu, Y. Wu, M. V. Reddy, et al. Long term cycling studies of electrospun TiO<sub>2</sub> nanostructures and their composites with MWCNTs for rechargeable Li-ion batteries, *Rsc Advances*, 2012, **2**, 531-537.

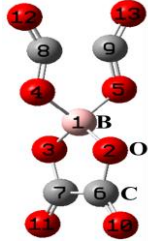
- [5] B. Li, M.Q. Xu, T.T. Li, W.S. Li, S.J. Hu. Prop-1-ene-1, 3-sultone as SEI formation additive in propylene carbonate-based electrolyte for lithium ion batteries, *Electrochem. Commun.*, 2012, **17**, 92-95.
- [6] E. G. Leggesse, J. C. Jiang, Theoretical study of the reductive decomposition of 1, 3-propane sultone: SEI forming additive in lithium-ion batteries, *Rsc Advances*, 2012, **2**, 5439-5446.
- [7] M.Q. Xu, Y.L. Liu, B. Li, W.S. Li, X.P. Li, S.J. Hu, Tris (pentafluorophenyl) phosphine: An electrolyte additive for high voltage Li-ion batteries, *Electrochem. Commun.*, 2012, **18**, 123-126.
- [8] Y. An, P. Zuo, C. Du, et al. Effects of VC-LiBOB binary additives on SEI formation in ionic liquid–organic composite electrolyte, *RSC Advances*, 2012, **2**, 4097-4102.
- [9] K. Xu, S.S. Zhang, R. Jow, Electrochemical impedance study of graphite/electrolyte interface formed in LiBOB/PC electrolyte, *J. Power Sources*, 2005, **143**, 197-202.
- [10] B.T. Yu, W.H. Qiu, F.S. Li, L.Cheng, Comparison of the electrochemical properties of LiBOB and LiPF<sub>6</sub> in electrolytes for LiMn<sub>2</sub>O<sub>4</sub>/Li cells, *J. Power Sources*, 2007, **166**, 499-502.
- [11] K. Xu, S.S. Zhang, T.R. Jow, LiBOB as Additive in LiPF<sub>6</sub>-Based Lithium Ion Electrolytes, *J. Electrochem. Solid-State Letters*, 2005, **8**, A365-A368.
- [12] S.S. Zhang, K. Xu, T.R. Jow, LiBOB-based gel electrolyte Li-ion battery for high temperature operation, *J. Power Sources*, 2006, **154**, 276-280.
- [13] M.S. Ding, T.R. Jow, Properties of PC-EA solvent and its solution of LiBOB comparison of linear esters to linear carbonates for use in lithium batteries, *J. Electrochem. Soc.*, 2005, **152**, A1199-A1207.
- [14] J. Hassouna, M. Wachtler, M. Wohlfahrt-Mehrens, B. Scrosati, Electrochemical behaviour of Sn and Sn–C composite electrodes in LiBOB containing electrolytes, *J. Power Sources*, 2011, **196**, 349-354.
- [15] J. Reitera, R. Dominkob, M. Nádherová, I. Jakubec, Ion-conducting lithium bis (oxalato) borate-based polymer electrolytes, *J. Power Sources*, 2009, **189**, 133-138.
- [16] J.-C. Panitz, U. Wietelmann, M. Wachtler, S. Strobele, M. Wohlfahrt-Mehrens, Film formation in LiBOB-containing electrolytes, *J. Power Sources*, 2006, **153**, 396-401.
- [17] X.Y. Li, Z.M. Xue, J.F. Zhao, C.H. Chen, A new lithium salt with tetrafluoro-1,2-benzenediolato and oxalato complexes of boron for lithium battery electrolytes, *J. Power Sources*, 2013, **253**, 274-279.
- [18] Idaho National Engineering and Environmental Laboratory, Partnership of New Generation Vehicle Battery Test Manui Revision3, U.S. Department of Energy DOE / ID 40597. 2001. 37
- [19] S.S. Zhang, Enhanced performance of Li-ion cell with LiBF<sub>4</sub>-PC based electrolyte by addition of small amount of LiBOB, *J. Power Sources*, 2006, **162**, 1379-1394.
- [20] K. Xu, U. Lee, S.S. Zhang, et al. Graphite/Electrolyte Interface Formed in LiBOB-Based Electrolytes II. Potential Dependence of Surface Chemistry on Graphitic Anodes, *J. Electrochem. Soc.*, 2004, **151**, A2106-A2112.

- [21] S. Dalavi, M.Q. Xu, B. Knight, B.L. Lucht, Effect of Added LiBOB on High Voltage ( $\text{LiNi}_{0.5}\text{Mn}_{1.5}\text{O}_4$ ) Spinel Cathodes, *J. Electrochem. Solid-State Letters*, 2012, **15**, A28-A31.
- [22] L. Yang, T. Markmaitree, B.L. Lucht, Inorganic additives for passivation of high voltage cathode materials, *J. Power Sources*, 2011, **196**, 2251-2254.
- [23] S.Y. Li, B.C. Li, X.L. Xu, X.M. Shi, Y.Y. Zhao, L.P. Mao, X.L. Cui, Electrochemical performances of two kinds of electrolytes based on lithium bis(oxalato)borate and sulfolane for advanced lithium ion batteries, *J. Power Sources*, 2012, **209**, 295-300.
- [24] K. Xu, Tailoring Electrolyte Composition for LiBOB, *J. Electrochem. Soc.*, 2008, **155**, A733-A738.
- [25] S. Wang, W.H. Qiu, T. Li, B.T. Yu, H.L. Zhao, Properties of Lithium bis(oxalato)borate (LiBOB) as a Lithium Salt and Cycle Performance in  $\text{LiMn}_2\text{O}_4$  Half Cell, *Int. J. Electrochem. Soc.*, 2006, **1**, 250-257.
- [26] S.Y. Ha, J.G. Han, Y.M. Song, M.J. Chun, S.I. Han, W.C. Shin, N.S. Choi, Using a lithium bis(oxalato) borate additive to improve electrochemical performance of high-voltage spinel  $\text{LiNi}_{0.5}\text{Mn}_{1.5}\text{O}_4$  cathodes at 60 °C, *Electrochim. Acta.*, 2013, **104**, 170-177.
- [27] K. Xu, B. Deveney, K. Nechev, Y. Lam, T.R. Jow, Evaluating LiBOB/Lactone Electrolytes in Large-Format Lithium-Ion Cells Based on Nickelate and Iron Phosphate, *J. Electrochem. Soc.*, 2008, **155**, A959-A964.
- [28] L.D. Xing, W.S. Li, C.Y. Wang, F.L. Gu, M.Q. Xu, C.L. Tan, J. Yi, Theoretical investigations on oxidative stability of solvents and oxidative decomposition mechanism of ethylene carbonate for lithium-ion battery use, *J. Phys. Chem. B*, 2009, **113**, 16596-16602.
- [29] L.D. Xing, C.Y. Wang, W.S. Li, M.Q. Xu, X.L. Meng, S.F. Zhao, Theoretical Insight into Oxidative Decomposition of Propylene Carbonate in the Lithium Ion Battery, *J. Phys. Chem. B*, 2009, **113**, 5181-5187.
- [30] T.T. Li, L.D. Xing, W.S. Li, Y.T. Wang, M.Q. Xu, F.L. Gu, S.J. Hu, How does Lithium Salt Anion Affect Oxidation Decomposition Reaction of Ethylene Carbonate: A Density Functional Theory Study, *J. Power Sources*, 2013, **244**, 668-674.
- [31] L.D. Xing, O. Borodin, G.D. Smith, W.S. Li, A Density Function Theory Study of the Role of Anions on the Oxidative Decomposition Reaction of Propylene Carbonate, *J. Phys. Chem. A*, 2011, **115**, 13896-13905.
- [32] L.D. Xing, O. Borodin, Oxidation Induced Decomposition of Ethylene Carbonate from DFT Calculations - Importance of Explicitly Treating Surrounding Solvent, *Phys. Chem. Chem. Phys.*, 2012, **14**, 12838-12843.
- [33] L.D. Xing, J. Vatamanu, O. Borodin, D. Bedrov, On the Atomistic Nature of Capacitance Enhancement Generated by Ionic Liquid Electrolyte Confined in Subnanometer Pores, *J. Phys. Chem. Lett.*, 2013, **14**, 132-140.
- [34] L.D. Xing, J. Vatamanu, G.D. Smith, D. Bedrov, Nanopatterning of Electrode Surfaces as a Route to Improved Energy Storage in Electrostatic Capacitors, *J. Phys. Chem. Lett.*, 2012, **3**,

---

1124-1129.

- [35] Y.T. Wang, L.D. Xing, O. Borodin, W.N. Huang, M.Q. Xu, X.P. Li, W.S. Li, Quantum chemistry study of the oxidation-induced stability and decomposition of propylene carbonate-containing complexes, *Phys. Chem. Chem. Phys.*, 2014, **16**, 6560-6567.
- [36] M.J. Frisch, G.W. Trucks, H.B. Schlegel, G.E. Scuseria, M.A. Robb, J.R. Cheeseman, G. Scalmani, V. Barone, B. Mennucci, G.A. Petersson, et al. Gaussian 09, Revision A, Gaussian, Inc., Wallingford, CT, 2009.
- [37] L.D. Xing, W.S. Li, M.Q. Xu, T.T. Li, L. Zhou, The reductive mechanism of ethylene sulfite as solid electrolyte interphase film-forming additive for lithium ion battery, *J. Power Sources*, 2011, **196**, 7044-7047.
- [38] S. Trasatti, The Absolute Electrode Potential: An Explanatory Note, *Pure Appl. Chem.*, 1986, **58**, 955-966.
- [39] L.D. Xing, J. Vatamanu, D. Bedrov, O. Borodin, G.D Smith, Electrode/ Electrolyte Interface in Sulfolane-Based Electrolytes for Li Ion Batteries: A Molecular Dynamics Simulation Study, *J. Phys. Chem. C*, 2012, 116:23871-23881.
- [40] K. Xu, Nonaqueous Liquid Electrolytes for Lithium-Based Rechargeable Batteries, *Chem. Rev.*, 2004, **104**, 4303-4417.
- [41] K. Xu, U. Lee, S. Zhang, et al. Graphite/Electrolyte Interface Formed in LiBOB-Based Electrolytes I. Differentiating the Roles of EC and LiBOB in SEI Formation, *J. Electrochem. Solid-State Letters*, 2004, **7**, A273-A277.
- [42] W.Q. Lu, Z.H. Chen, H. Joachin, J. Prakash, J. Liu, K. Amine, Thermal and electrochemical characterization of MCMB/LiNi<sub>1/3</sub>Co<sub>1/3</sub>Mn<sub>1/3</sub>O<sub>2</sub> using LiBoB as an electrolyte additive, *J. Power Sources*, 2007, **163**, 1074-1079.
- [43] F. Joho, P. Novak, SNIFTIRS investigation of the oxidative decomposition of organic -carbonate-based electrolytes for lithium-ion cells, *Electrochim. Acta.*, 2000, **45**, 3589-3599.
- [44] M. Onuki, S. Kinoshita, Y. Sakata, M. Yanagidate, Y. Otake, M. Ue, Deguchi M. Identification of the Source of Evolved Gas in Li-Ion Batteries Using <sup>13</sup>C-labeled Solvents, *J. Electrochem. Soc.*, 2008, **155**, A794-A797.
- [45] R.Mogi, M. Inaba, Y. Iriyama, T. Abe, Z. Ogumi, Study on the decomposition mechanism of alkyl carbonate on lithium metal by pyrolysis-gas chromatography-mass spectroscopy, *J. Power Sources*, 2003, **119-121**, 597-603.

Table 1 NPA Atomic charges of BOB<sup>-</sup> before and after oxidation.


	Isolated BOB <sup>-</sup>		EC-BOB <sup>-</sup>		PC-BOB <sup>-</sup>		DMC-BOB <sup>-</sup>	
	Before	After	Before	After	Before	After	Before	After
1 B	1.20242	1.22223	1.20287	1.22263	1.20258	1.22252	1.20272	1.22338
2 O	-0.68142	-0.68373	-0.67871	-0.68090	-0.68014	-0.68136	-0.68018	-0.68251
3 O	-0.68152	-0.68373	-0.67830	-0.68060	-0.67850	-0.68098	-0.68247	-0.68198
4 O	-0.68151	-0.57852	-0.68150	-0.57883	-0.68157	-0.57844	-0.68404	-0.58338
5 O	-0.68143	-0.57852	-0.68144	-0.57898	-0.68131	-0.57892	-0.68044	-0.58341
6 C	0.71564	0.72080	0.71603	0.72160	0.71549	0.72222	0.71574	0.72078
7 C	0.71569	0.72080	0.71756	0.72292	0.71784	0.72263	0.71468	0.72004
8 C	0.71569	0.83460	0.71577	0.83547	0.71573	0.83531	0.71626	0.83814
9 C	0.71564	0.83460	0.71575	0.83544	0.71583	0.83499	0.71668	0.83808
10 O	-0.58486	-0.53628	-0.58592	-0.53811	-0.58433	-0.53919	-0.58569	-0.53931
11 O	-0.58474	-0.53628	-0.58757	-0.54064	-0.58876	-0.53980	-0.58461	-0.53907
12 O	-0.58475	-0.36798	-0.58381	-0.36726	-0.58443	-0.36733	-0.58595	-0.37200
13 O	-0.58485	-0.36798	-0.58389	-0.36730	-0.58403	-0.36751	-0.58515	-0.37201

**Figure captions:**

**Figure 1** Optimized structures of isolate carbonates, carbonate-BOB<sup>-</sup> and carbonate-PF<sub>6</sub><sup>-</sup> clusters before and after oxidation (-e), together with the calculated oxidation potentials (V vs. Li<sup>+</sup>/Li). Sum of NPA charge of the oxidized clusters in red and blue circle is relative to 0 and -1 e, respectively.

**Figure 2** Optimized structures and geometric parameters (bond length in Å, dihedral angle in degree, relative free energy in kJ/mol) of the stationary points and the transition states (TSs) for the oxidative decomposition of isolate BOB<sup>-</sup>.

**Figure 3** Optimized structures of the stationary points and the transition states (TSs) for the oxidative decomposition reactions of EC-BOB<sup>-</sup>-e cluster.

**Figure 4** Relative free energy of oxidative decomposition of BOB<sup>-</sup>-e and EC-BOB<sup>-</sup>-e clusters (from Path1 to Path 7).

**Figure 5** Possible polymerization reactions and relative free energies (kJ/mol) of R1.



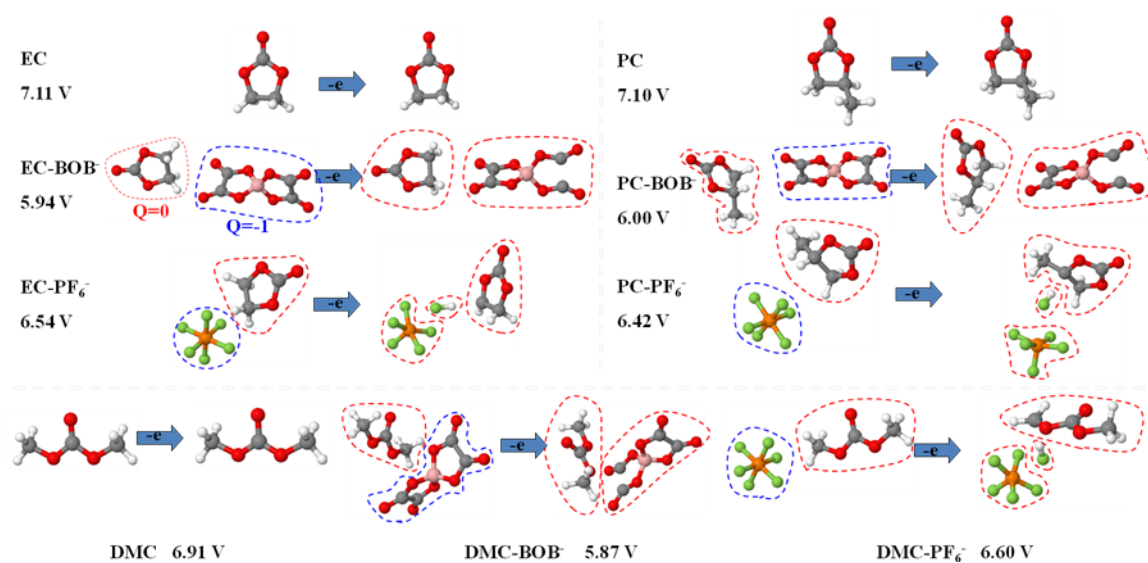


Figure 1 Optimized structures of isolate carbonates, carbonate-BOB<sup>-</sup> and carbonate-PF<sub>6</sub><sup>-</sup> clusters before and after oxidation (-e), together with the calculated oxidation potentials (V vs. Li<sup>+</sup>/Li).

Sum of NPA charge of the oxidized clusters in red and blue circle is relative to 0 and -1 e, respectively.

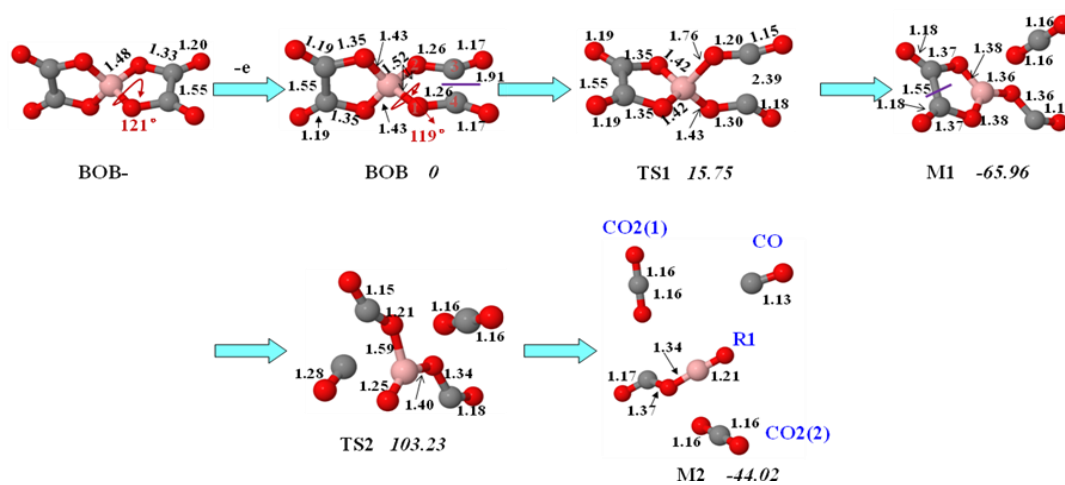


Figure 2 Optimized structures and geometric parameters (bond length in Å, dihedral angle in degree, relative free energy in kJ/mol) of the stationary points and the transition states (TSs) for the oxidative decomposition of isolate BOB<sup>-</sup>.

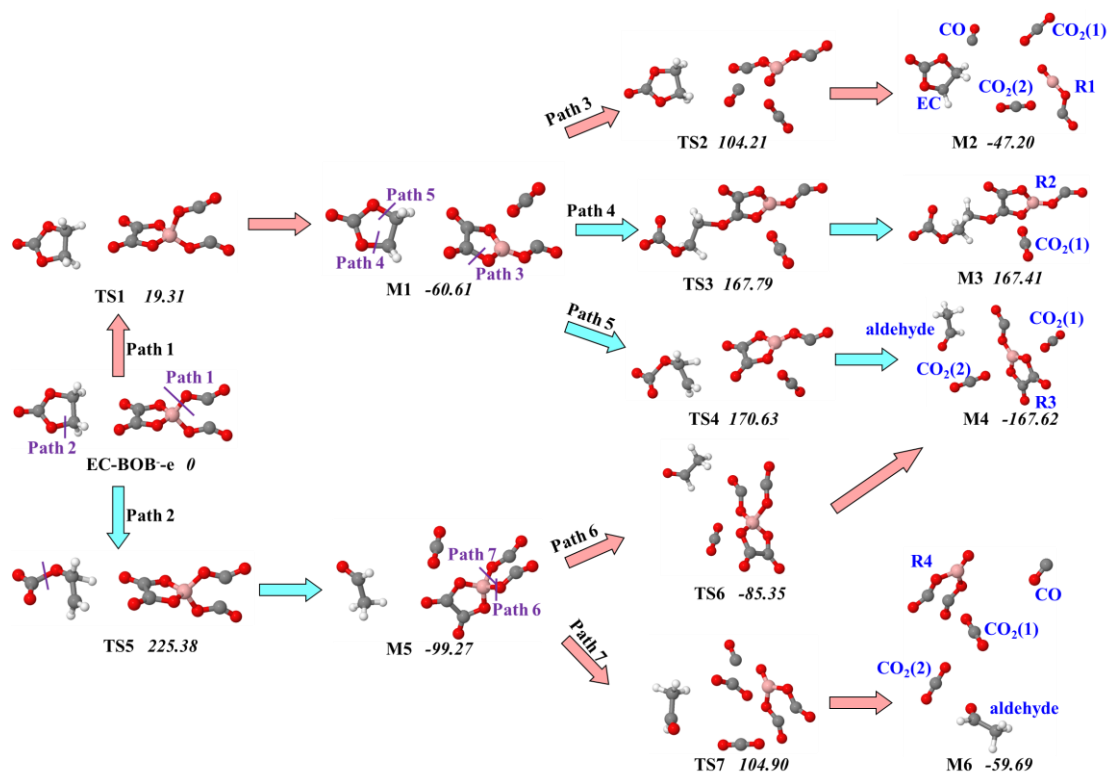


Figure 3 Optimized structures of the stationary points and the transition states (TSs) for the oxidative decomposition reactions of EC-BOB<sup>-e</sup> cluster.

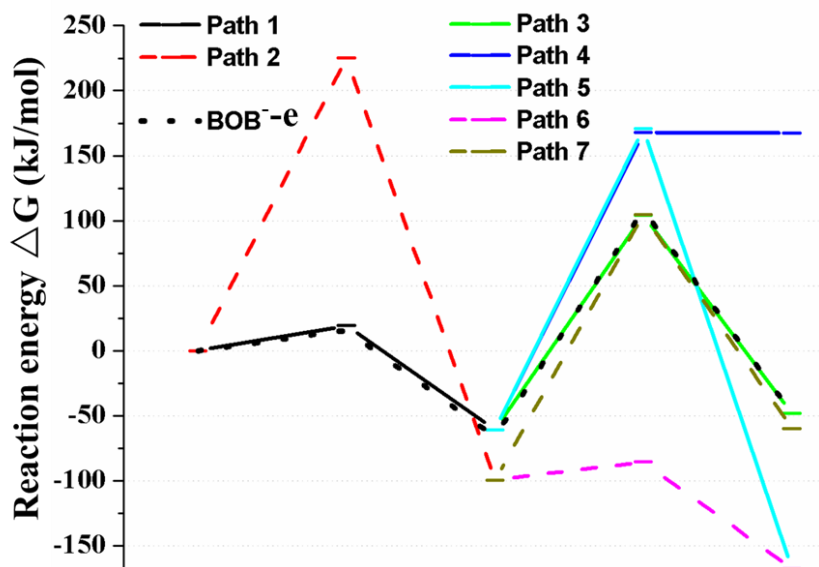


Figure 4 Relative free energy of oxidative decomposition of BOB<sup>-e</sup> and EC-BOB<sup>-e</sup> clusters (from Path1 to Path 7).

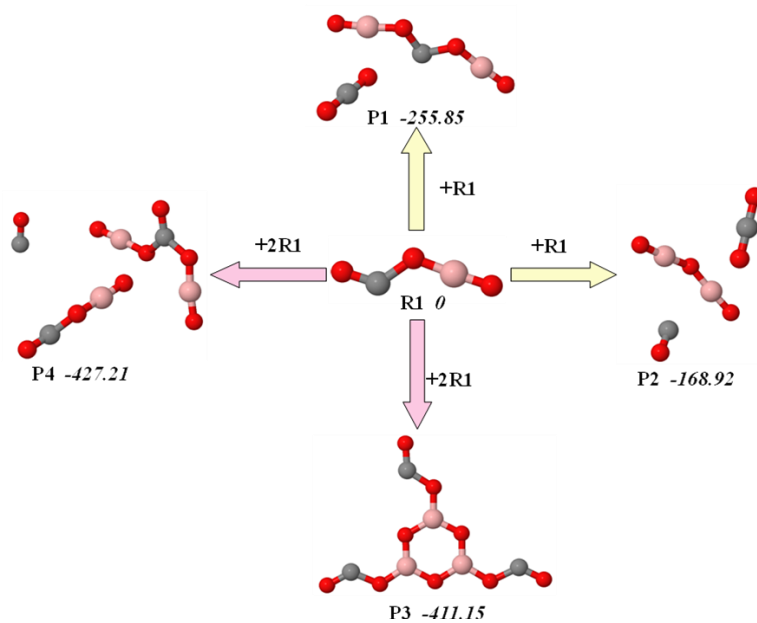
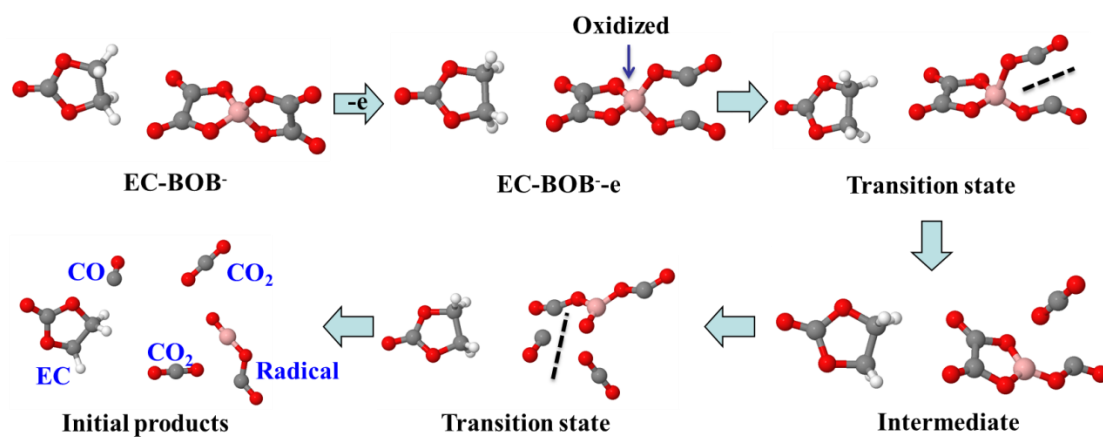


Figure 5 Possible polymerization reactions and relative free energies (kJ/mol) of R1.



The most possible oxidative decomposition reaction path of EC-BOB<sup>-</sup> cluster.